Nanoscale Motors Powered by Catalytic Reactions

NSF NIRT Grant CTS-0506967

PIs: **Ayusman Sen,* Thomas Mallouk, Jeffrey Catchmark, Vincent Crespi**
The Pennsylvania State University
*E-mail: asen@psu.edu

This research involves a four-year collaborative effort to study a novel class of nano/microscale motors and pumps which are powered by catalytic reactions that convert chemical energy to mechanical motion. The planned studies will provide a scientific underpinning for future applications of catalytically driven motion on the nanometer length scale. In the past year, we have focused on (a) achieving spatial and temporal control of motion, (b) the observation of chemotaxis, i.e. the directed movement of catalytic nano-objects towards region of higher fuel concentration, and (c) the attachment of cargo to nanomotors and their transportation. Our results in each of these areas are briefly described below [1].

Reversible Pattern Formation Through Photolysis [2]. We have recently described catalytically-induced motion at the nano/microscale, some which involves ion gradients, in non-biological systems. However, while spatial control has been achieved over fluid movement and pattern formation through such a process, the lack of an "on/off" switch prevented reversible temporal control.

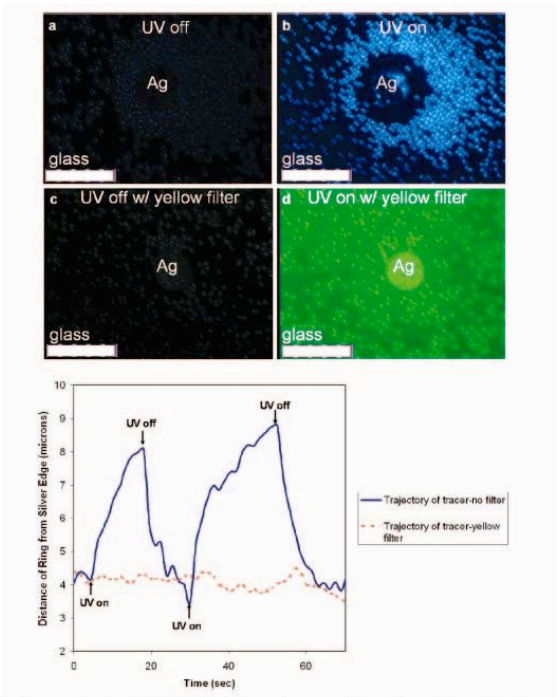

Figure 1. (top) UV light-induced reversible pattern formation in the presence of a spatially defined silver catalyst (Ag) on silicon dioxide (a) before and (b) after opening the aperture. (c) The absence of patterning when a UV absorbing filter is placed in the light path before and (d) after opening the aperture. Scale bar represents 40 μm. (bottom) Trajectory of tracers around silver disk without (solid line) and with (dashed line) a UV absorbing yellow filter in place. No filter results in dynamic patterning in the presence of an open aperture (UV on) which relaxes upon closing the aperture (UV off), whereas in the presence of a filter the tracers are indifferent to UV irradiation.

We have now succeeded in achieving *both* spatial and temporal control over movement and patterning at the micron-scale using photolytically-generated ion gradients (Fig. 1). The patterning appears to arise from the formation of silver (Ag^+) and hydroperoxide (OOH^-) ions by photolytic decomposition of hydrogen peroxide (H_2O_2) at a silver feature. The difference in diffusion coefficients between these two ions establishes a diffusion-induced electric field that is responsible for the observed duffusiophoretic motion of tracer particles. This mechanism differs from the previously reported electrokonetically-driven flow that requires the presence of two different metals in contact and that occurs in the absence of light.

Chemotaxis of Catalytic Nanorods. We have observed the first example of chemotaxis outside biological systems. This allows the use of catalytic nanorods in directional transportation, but also helps to elucidate the mechanism involved in bacterial chemotaxis by creating a non-biological analog.

The PtAu nanorods are known to move in hydrogen peroxide (H_2O_2) solution with a speed that is proportional to the concentration of H_2O_2. Thus, we reasoned that PtAu rods would move towards higher H_2O_2 concentration in a concentration gradient. A [H_2O_2] gradient was

created by using a hydrogel soaked with 30% H_2O_2. The gel was put in the center of an imaging chamber, which was sealed after the injection of nanorod solution in pure water. The chemotaxis of these PtAu rods was observed under an optical microscope. The graph (Fig. 2) on the left shows relatively even distribution of rods at 0.7 h, while the one on the right shows a dramatic increase of rod density near the gel at 110 h. This phenomenon however, was not observed with control experiments with (a) Au rods in 30-0% H_2O_2 gradient, and (b) PtAu rods in pure water only (no gradient).

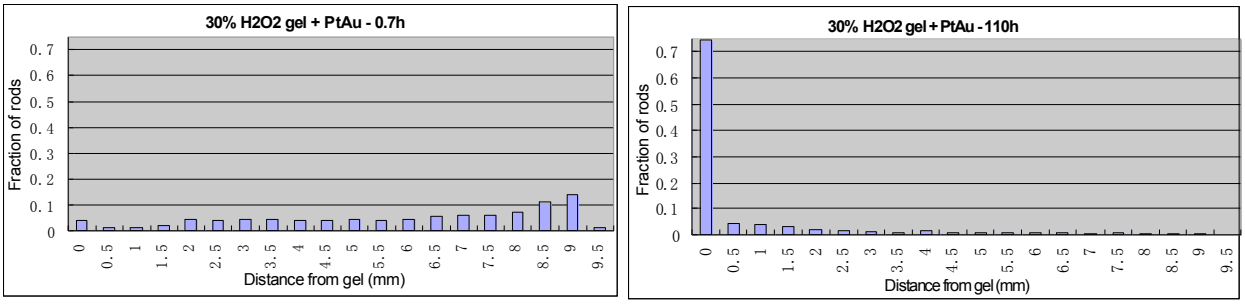

Figure 2. Distribution of PtAu rods (2 μm long, 400 nm diameter) as a function of time. After 0.7 h (left) and after 110 h (right). The rods were initially in pure water and exposed to hydrogel with 30 wt% H_2O_2 on the left.

Cargo Transport by Catalytic Nanorods. PtAu nanorods exhibit autonomous motion towards the Pt end in the presence H_2O_2 fuel solution. Applications for self-propelled nanomotors include: self-assembly of super structures, roving sensors and site-directed drug delivery. These applications require the attachment of a functional nano/microscale 'cargo' to the motor and the PtAu/H_2O_2 system may be used as a prototype to test the feasibility of using these rods for the above mentioned applications.

Initially, electrostatic force was used to attach positively charged polystyrene (PS) microspheres (1-2 μm) to negatively charged polypyrrole segment at the end of the nanorods (2-3 μm long, 400 nm diameter) (Fig. 3). This mode however, does not always afford selective attachment of cargo to the tip of the rods necessary to ensure translation of rods and to minimize the drag force. To improve the selectivity of attachment, a self-assembled monolayer of biotin terminated disulfides was formed at the Au tips of the rods. Subsequently, the biotin-streptavidin linkage was used to attach streptavidin coated microspheres, and this method gave higher yields of heterodoublets with the desired geometry. Table 1 shows the effect of attaching cargo of 1 μm and 2 μm diameters. While comparison among batches is not feasible due to large variations in PtAu nanomotor speeds, within each batch, the rods slow down upon attachment of cargo.

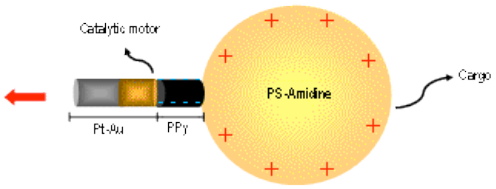

Figure 3. Pt-Au-PPy catalytic motor with amidine cargo attached in at the tip.

The theoretical arm of the catalytic motors project works with the experimental efforts, attempting to model and analyze experiments to gain a deeper understanding of the phenomena and to suggest new experiments and ultimately, applications. Rods typically attach to the cargo in a skewed configuration. This misalignment is actually very useful because it imparts a significant rotational component to the doublets' motion that is absent in the case of rods alone (Fig. 4). The resulting torque, superimposed on the translational force, and their respective effects on the fluidic resistance give us independent measures of the motive effects

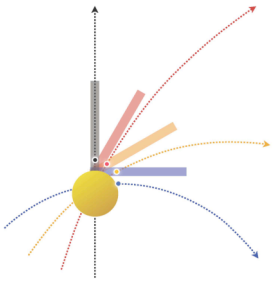

Figure 4. Trajectories for rods attached to cargo in different configurations

generated by the rods. Having direct experimental access to both a motive force and a motive torque gives us a means to spatially resolve the motor activity, since the torque depends upon the spatial distribution of the force across the surface of the composite rod-sphere particle. The hydrodynamics in these experiments is more complex than in the earlier investigations, because of the more complex shapes of the composite rod-sphere particles. We are currently extending our analysis to calculate the flows in this new setting.

Table 1: The effect of cargo size on catalytic nanomotor speed

Cargo Attachment By Electrostatic Interaction		
Cargo Size (μm)	Avg. Speed (μm/s)	Directionality
0	12.9 ± 3.1	0.6 ± 0.3
1	7.6 ± 2.2	0.7 ± 0.1
2	5.3 ± 1.0	0.6 ± 0.2
Cargo Attachment By Biotin-Streptavidin Interaction		
Cargo Size (μm)	Avg. Speed (μm/s)	Directionality
0	7.3 ± 1.5	0.3 ± 0.2
1	6.1 ± 1.6	0.3 ± 0.2
2	4.2 ± 0.9	0.5 ± 0.3

References

[1] For further information about this project link to http://research.chem.psu.edu/axsgroup/research-nanomotors.html or email: asen@psu.edu
[2] Timothy R. Kline and Ayusman Sen, "Reversible Pattern Formation Through Photolysis," *Langmuir*, **2006**, *22*, 7124.